PAPER NO. AAS 77-116

ANALYTIC INVESTIGATION OF THE AEM-A/HCMM ATTITUDE CONTROL SYSTEM PERFORMANCE

by

G. M. LERNER, W. HUANG
and M. D. SHUSTER

Computer Sciences Corporation
Silver Spring, Maryland

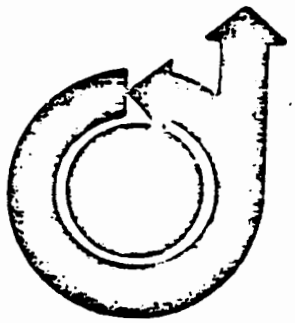

AAS/AIAA Astrodynamics Conference

SEPTEMBER 7–9, 1977
GRAND TETON NATIONAL PARK, WYOMING

ANALYTIC INVESTIGATION OF THE AEM-A/HCMM ATTITUDE CONTROL SYSTEM PERFORMANCE*

G. M. Lerner,† W. Huang,† and M. D. Shuster†

The Heat Capacity Mapping Mission (HCMM), scheduled for launch in 1978, will be three-axis stabilized relative to the Earth in a 600-kilometer altitude, polar orbit. The autonomous attitude control system consists of three torquing coils and a momentum wheel driven in response to error signals computed from data received from an infrared horizon sensor and a magnetometer. This paper presents a simple model of the attitude dynamics and derives the equations that determine the stability of the system during both attitude acquisition (acquisition-mode) and mission operations (mission-mode). Modifications to the proposed mission-mode control laws which speed the system's response to transient attitude errors and reduce the steady-state attitude errors are suggested. Numerical simulations are performed to validate the results obtained with the simple model.

*Work supported by the Attitude Determination and Control Section, Goddard Space Flight Center, National Aeronautics and Space Administration, under Contract No. NAS 5-11999.

†Member, Technical Staff, System Sciences Division, Computer Sciences Corporation, Silver Spring, Maryland 20910.

INTRODUCTION

The Heat Capacity Mapping Mission (HCMM), scheduled for launch in the second quarter of 1978, is the first of the Applications Explorer Missions (AEM). The AEM, which use relatively small spacecraft, provide a means for performing various tasks that require low cost and quick reaction. To make a thermal map of North America, the HCMM satellite will be placed into a circular, Sun-synchronous orbit at a 600-kilometer altitude and a 98-degree inclination.* It will be three-axis stabilized, with the spacecraft's y- and z-axes along the negative orbit normal and nadir, respectively. The HCMM attitude control system consists of an integrated infrared horizon sensor/momentum wheel assembly or scanwheel® (registered trademark of ITHACO, Inc.), mounted along the spacecraft's negative y-axis, and three-orthogonal fluxgate magnetometers and electromagnetic torquing coils. Elegantly simple control laws, based on a proposal by Seymor Kant, Peter Hui, and Joseph Lidston of Goddard Space Flight Center and described in Reference 1, are used to despin the spacecraft after separation (rate capture), to orient the scanwheel angular momentum vector to within 10 degrees of orbit normal (attitude capture), to achieve Earth lock and operational wheel speed (pitch capture and momentum control), and to maintain pitch and roll within 1 degree of zero.†

The performance of these control laws has been the subject of several investigations (References 1 and 2). However, the equations that describe the attitude dynamics are intractable and, consequently, the earlier work relies heavily on numerical simulations and obtains largely phenomenological results. This paper presents a simple analytic model for the attitude motion of the HCMM satellite whose solutions retain all the features of the complete simulated dynamics. Within such a model, it is possible to study in a fundamental way the

*The ascending node will occur at 2 p.m. local time.

†Yaw is maintained within 2 degrees of zero by gyrocompassing.

performance of the HCMM acquisition- and mission-mode attitude control laws. In particular, the stability conditions of the system in both modes assume relatively simple analytic forms from which can be obtained insight into the dependence of stability on the spacecraft and control law parameters. These results are not easily obtained from numerical simulations. This semiquantitative model does, in fact, suggest modifications to the mission-mode control law which result in improved attitude control performance.

MAGNETIC FIELD MODEL

The spacecraft is assumed to be in a circular, polar orbit, and the Earth's magnetic field is taken to be a pure magnetic dipole with the magnetic South Pole coinciding with the geographic North Pole.* The magnetic field at the spacecraft in the orbital reference frame, denoted by the subscript O , ($\hat{e}_x$ = velocity direction; $\hat{e}_y$ = negative orbit normal; $\hat{e}_z$ = nadir direction) is then

$$\vec{B}_O(t) = B\,(\cos \omega_o t\, \hat{e}_x + 2 \sin \omega_o t\, \hat{e}_z) \tag{1}$$

where $\omega_o = 0.00108$ radians per second is the orbital angular velocity and $B = 2.3 \times 10^{-5}$ Wb/m^2 at a 600-kilometer altitude. The spacecraft is assumed to be traveling northward at the equator at $t = 0$. The magnetic field may be written in the inertial reference frame, denoted by the subscript I , ($\hat{z}$ = Earth's spin axis; $\hat{x}$ = descending node; $\hat{y}$ = orbit normal) by substituting

$$\begin{aligned} \hat{e}_x &= \cos \omega_o t\, \hat{z} + \sin \omega_o t\, \hat{x} \\ \hat{e}_z &= -\sin \omega_o t\, \hat{z} + \cos \omega_o t\, \hat{x} \end{aligned} \tag{2}$$

*The south end of the dipole is actually located at 78.6° N latitude. The error in the field magnitude for HCMM, as derived from the dipole model, is about 4 percent at the equator.

into Equation (1) to obtain

$$\vec{B}_I(t) = \frac{3}{2} B \left\{ \sin 2\omega_o t \, \hat{x} + \left(\cos 2\omega_o t - \frac{1}{3} \right) \hat{z} \right\} \qquad (3)$$

ACQUISITION-MODE CONTROL LAW

The rate and attitude capture control law drives the three electromagnets in response to the rate of change of the magnetic field as measured by the magnetometers in the spacecraft reference frame, denoted by the subscript B or body coordinates. The actual control law has the form*

$$\vec{D}_B = -k' \, \mathrm{sgn} \, (\dot{\vec{B}}_B) \qquad (4a)$$

where $\vec{D}_B$ is the commanded magnetic dipole moment and $\vec{B}_B$ is the magnetic field, both measured in body coordinates, and $k' = 10$ A-m^2 (10,000 pole-cm).

The control law in the model presented here is taken as

$$\vec{D}_B = -k \dot{\vec{B}}_B \qquad (4b)$$

where the discrete sgn function has been replaced by a continuous function and k is chosen so that $\vec{D}_B$ assumes similar values in Equations (4a) and (4b). The advantage of this approximation is that it allows an analytic solution of the equations of motion. Numerical simulations with the "bang-bang" control law of Equation (4a) give results which are similar to those with the proportional control law of Equation (4b).

---

* $\mathrm{sgn}\,(x) \equiv \begin{cases} +1 \text{ if } x \geq 0 \\ -1 \text{ if } x < 0 \end{cases}$

In inertial coordinates, Equation (4b) may be rewritten as

$$\vec{D}_I = A^T \vec{D}_B = -k\left(\dot{\vec{B}}_B\right)_I = -k\,(\dot{\vec{B}}_I - \vec{\omega} \times \vec{B}_I) \tag{5}$$

where the orthogonal attitude (or direction cosine) matrix A transforms vectors from inertial to body coordinates and $\vec{\omega} = (\omega_x, \omega_y, \omega_z)^T$ is the angular velocity of the spacecraft relative to the inertial reference frame. The capture control torque in inertial coordinates is

$$\vec{N}_I^C = \vec{D}_I \times \vec{B}_I = -k\left[\dot{\vec{B}}_I \times \vec{B}_I - (\vec{\omega} \cdot \vec{B}_I)\,\vec{B}_I + B_I^2\,\vec{\omega}\right] \tag{6}$$

or explicitly

$$\vec{N}_I^C = \frac{9kB^2}{4}\begin{bmatrix} -\left(\frac{1}{3} - \cos 2\omega_o t\right)^2 \omega_x - \sin 2\omega_o t\left(\frac{1}{3} - \cos 2\omega_o t\right)\omega_z \\ 2\left(1 - \frac{1}{3}\cos 2\omega_o t\right)\omega_o - 2\left(\frac{5}{9} - \frac{1}{3}\cos 2\omega_o t\right)\omega_y \\ -\sin 2\omega_o t\left(\frac{1}{3} - \cos 2\omega_o t\right)\omega_x - \sin^2 2\omega_o t\,\omega_z \end{bmatrix} \tag{7}$$

Euler's equation for an (assumed) spherically symmetric spacecraft takes the form

$$I\dot{\vec{\omega}} + \dot{\vec{H}}_I = \vec{N}_I^C + \vec{N}_I^E \tag{8}$$

where

$$\vec{H}_I = A^T\,(0, -h, 0)^T \tag{9}$$

is the wheel angular momentum in inertial coordinates, I is the spacecraft's moment of inertia, $\vec{N}_I^E$ is the sum of the environmental disturbance torques, and h is the magnitude of the wheel angular momentum.

The qualitative effect of the control law depends on the magnitude of the spacecraft's angular velocity, $\vec{\omega}$, relative to the orbital angular velocity, ω_o. The two regions, $|\vec{\omega}| >> \omega_o$ and $|\vec{\omega}| \leq \omega_o$, are denoted rate and attitude capture, respectively.

Let us first consider the situation at spacecraft separation where $|\vec{\omega}| >> \omega_o$ and thus $|\vec{\omega} \times \vec{B}_I| >> |\dot{\vec{B}}_I|$. Ignoring the environmental torques and the effect of the wheel angular momentum for the moment, Equation (8) may be written as

$$I \dot{\vec{\omega}} + k [\vec{\omega} B_I^2 - (\vec{\omega} \cdot \vec{B}_I) \vec{B}_I] = 0 \qquad (10)$$

Thus, the component of $\vec{\omega}$ perpendicular to $\vec{B}_I$ decays with a time constant proportional to $|\vec{B}_I|^2$. The orbital motion ensures that $\vec{\omega}$ cannot remain parallel to $\vec{B}_I$ (there are no such torques), and so all components of $\vec{\omega}$ in inertial coordinates decay until $|\vec{\omega}| \approx \omega_o$. The effect of the wheel angular momentum is to superimpose oscillations at the nutation frequency, $\omega_n >> \omega_o$, on the exponential decay of $\vec{\omega}$.

After $|\vec{\omega}|$ is reduced to approximately the orbital angular velocity, the change in the magnetic field due to the orbital motion, $\dot{\vec{B}}_I$, can no longer be neglected. The approximate steady-state motion may be deduced by setting $\langle \vec{N}_I^C \rangle = 0$ in Equation (7) to obtain a solution

$$\langle \omega_x^{ss} \rangle \approx \langle \omega_z^{ss} \rangle \approx 0$$
$$\langle \omega_y^{ss} \rangle \approx \frac{9}{5} \omega_o \qquad (11)$$

where the superscript denotes the approximate steady-state solution and the brackets denote that the coefficients in Equation (7) have been orbit averaged. Thus, the steady-state attitude rate is about the orbit normal at approximately twice the orbital rate.

Now consider the steady-state attitude. Initially, the wheel angular momentum vector, $\vec{H_I}$, may have any orientation relative to the orbit normal. The control torque causes $\vec{H_I}$ to precess about the orbit normal to satisfy Equation (11). This results, on the orbit average, in the continuous subtraction of angular momentum from the inertial x- and z-axes and the addition of angular momentum to the inertial y-axis (orbit normal). Because $|\vec{H_I}| = h$, by control of the wheel speed, the steady-state attitude is with the wheel angular momentum along the orbit normal. The antiparallel attitude (with the wheel angular momentum along the negative orbit normal) is a saddle point or a position of unstable equilibrium because any perturbation results in the addition to the system of angular momentum about the orbit normal. Figure 1 provides a qualitative illustration of the effect of the control law.

To quantify these arguments, we explicitly solve Euler's equations for small perturbations from the nominal attitude. The matrix that transforms vectors from orbital to body coordinates is

$$K = \begin{bmatrix} 1 & y & -p \\ -y & 1 & r \\ p & -r & 1 \end{bmatrix} \qquad (12)$$

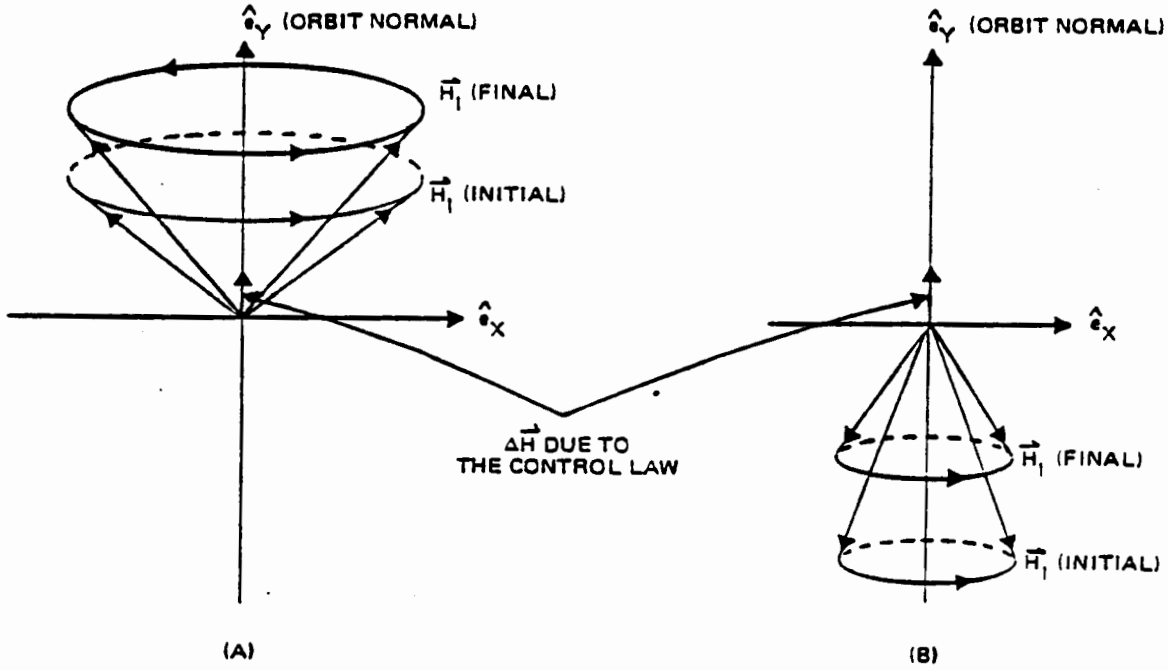

Fig. 1 The orbital motion causes the wheel angular momentum vector to precess in a cone about the orbit normal. The control law adds angular momentum along the orbit normal and removes angular momentum in the orbit plane. Regardless of the initial orientation, $\vec{H}_I$ migrates to the orbit normal.

where roll (r), pitch (p), and yaw (y) denote small angles about the orbital reference axes, $\hat{e}_x$, $\hat{e}_y$, and $\hat{e}_z$. The control torque in body coordinates is

$$\vec{N}_B^C = -k \frac{d}{dt}[K\vec{B}_O(t)] \times [K\vec{B}_O(t)]$$

$$\approx -kB^2 \begin{bmatrix} 2\omega_o y + 4\dot{r} \sin^2 \omega_o t - \dot{y} \sin 2\omega_o t \\ 2\omega_o + \dot{p} (\cos^2 \omega_o t + 4\sin^2 \omega_o t) \\ -2\omega_o r + \dot{y} \cos^2 \omega_o t - \dot{r} \sin 2\omega_o t \end{bmatrix} \tag{13}$$

Hence Euler's equation may be written in body coordinates as

$$I\dot{\vec{\omega}} + \vec{\omega} \times \vec{H}_B = \vec{N}_B^C \tag{14}$$

where the environmental disturbance torques are assumed to be negligible during attitude acquisition. Substituting Equation (13) into Equation (14) and using the expressions for the angular velocity and body angular momentum, $\vec{\omega} = (\dot{r} - \omega_o y, \dot{p} - \omega_o, \dot{y} + \omega_o r)^T$ and $\vec{H}_B = (0, -h, 0)^T$, we obtain the result

$$I\ddot{r} + (h - I\omega_o)\,\dot{y} + h\omega_o r + kB^2\,(2\omega_o y + 4\dot{r}\sin^2\omega_o t - \dot{y}\sin 2\omega_o t) = 0 \qquad (15a)$$

$$I\ddot{p} + \frac{9kB^2}{2}\left(\frac{5}{9} - \frac{1}{3}\cos 2\omega_o t\right)\dot{p} + 2kB^2\omega_o = 0 \qquad (15b)$$

$$I\ddot{y} - (h - I\omega_o)\,\dot{r} + h\omega_o y + kB^2\,(-2\omega_o r + \dot{y}\cos^2\omega_o t - \dot{r}\sin 2\omega_o t) = 0 \qquad (15c)$$

where $h > 0$ if the final orientation of the wheel angular momentum is parallel to the orbit normal and $h < 0$ if it is antiparallel to the orbit normal.

The pitch equation is decoupled from roll and yaw, which are coupled through the momentum wheel. The Fourier series solution for pitch rate is given in the Appendix and may be averaged over the orbit to obtain

$$\langle \dot{p}_{ss} \rangle = \frac{\omega_o}{5}\left[4 + 8\sum_{m=1}^{\infty}(-)^{m+1}\,\frac{m^2}{a^2 + m^2}\,I_m^2(b)\right] \qquad (16)$$

where

$$a = \frac{5\omega_1}{9\omega_o}$$

$$b = \frac{\omega_1}{3\omega_o} \qquad (17)$$

$$\omega_1 = \frac{9k\,B^2}{4\,I}$$

and I_m are modified Bessel functions of the first kind (Reference 3). Note that the steady-state mean pitch rate is neither ω_o which is the $\omega_1 \to \infty$ ("strong-coupling") limit and may be obtained by assuming that the spacecraft tracks the magnetic field nor $\frac{4}{5}\omega_o$ which is the $\omega_1 \to 0$ ("weak-coupling") limit and may be obtained directly from Equation (15b). Equation (16) is an infinite series whose terms alternate in sign. For $b \gg m \gg 1$

$$I_m(b) \sim \frac{\exp(b)}{\sqrt{2\pi b}}\,(1 + O(m/b)) \qquad (18)$$

Thus, for large b convergence is very poor and the series in Equation (16) must be summed with care. Figure 2 shows the steady-state mean pitch rate as a function of ω_1. In Equation (16), twelve terms were required to obtain 0.1 percent accuracy for $\omega_1 = 30\omega_o$. Note that $\langle \dot{p}_{ss} \rangle$ satisfies the inequality

$$\frac{4}{5}\omega_o \le \langle \dot{p}_{ss} \rangle \le \omega_o \qquad (19)$$

For HCMM, $\omega_1 \approx 6\omega_o$; thus, $\langle \dot{p}_{ss} \rangle = 0.96\,\omega_o$.

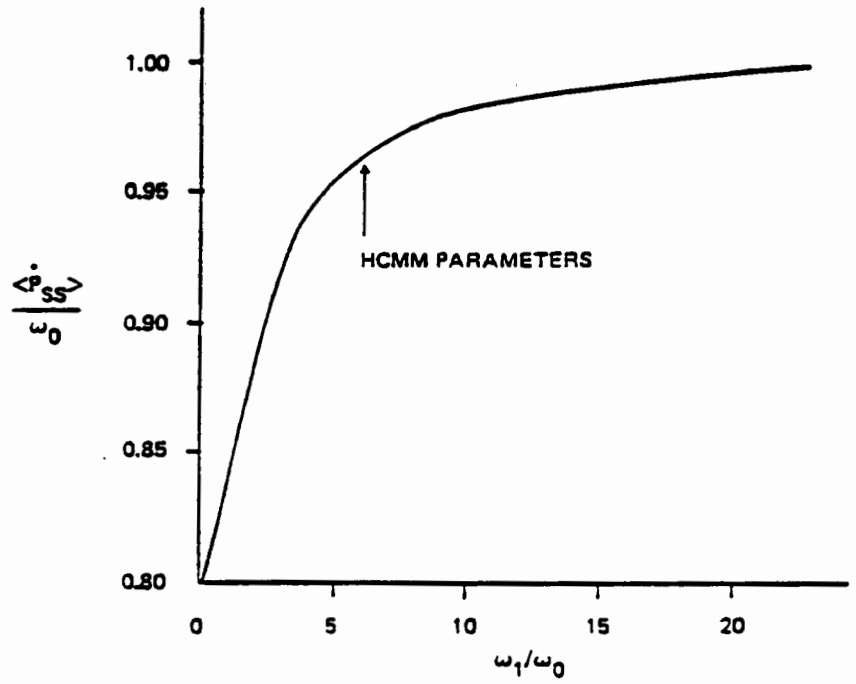

Fig. 2 Steady State Mean Pitch Rate

The roll and yaw equations may be written approximately in Laplace transform notation as

$$\left[\begin{array}{c|c} I S^2 + 2k B^2 S + h\omega_o & (h - I\omega_o) S + 2k B^2 \omega_o \\ \hline -(h - I\omega_o) S - 2k B^2 \omega_o & I S^2 + \frac{1}{2} k B^2 S + h\omega_o \end{array}\right] \left[\begin{array}{c} L(r) \\ L(y) \end{array}\right] = \left[\begin{array}{c} L(N_{Ex}) \\ L(N_{Ey}) \end{array}\right] \qquad (20)$$

where $\sin 2\omega_o t$, $\sin^2 \omega_o t$, and $\cos^2 \omega_o t$ have been replaced with their orbit-averaged values $\langle \sin 2\omega_o t \rangle = 0$, and $\langle \sin^2 \omega_o t \rangle = \langle \cos^2 \omega_o t \rangle = \frac{1}{2}$.

The characteristic equation for the eigenvalues of the above matrix is

$$I^2 S^4 + \frac{5k B^2 I}{2} S^3 + \left[h^2 + (I\omega_o)^2 + (k B^2)^2\right] S^2 + \left[\frac{13}{2} k B^2 h\omega_o - 4k B^2 I\omega_o^2\right] S + h^2 \omega_o^2 + (2\omega_o k B^2)^2 = 0 \quad (21)$$

from which the stability conditions of the system may be determined. A necessary condition for asymptotic stability is that all the coefficients in Equation (21) are positive. Hence,

$$h > \frac{8}{13} I\omega_o > 0 \quad (22a)$$

$$k > 0 \quad (22b)$$

The requirement that $h > 0$ demonstrates that only the attitude with the wheel angular momentum parallel to the orbit normal can be stable. Sufficient conditions for stability are obtained by applying Routh's criteria (Reference 4) to Equation (21). This leads to the inequality

$$\frac{13}{2} h^3 - \frac{117}{5} h^2 I\omega_o + \frac{273}{5} h(I\omega_o)^2 - \frac{52}{5} (I\omega_o)^3 > (k B^2)^2 (14 I\omega_o - \frac{13}{2} h) \quad (23)$$

Assuming a maximum dipole strength of 10 $A \cdot m^2$ (10,000 pole cm), the constants for HCMM are

$$\begin{aligned} 3k B\omega_o &\approx 10 \text{ A} \cdot \text{m}^2 \\ I\omega_o &\approx 0.024 \text{ J} \cdot \text{s} \\ h &\approx 5.2 \text{ J} \cdot \text{s} \\ k B^2 &\approx 0.072 \text{ J} \cdot \text{s} \end{aligned} \quad (24)$$

which can be seen to satisfy Equations (22) and (23).

A series of numerical simulations was run to investigate the validity of the stability equations. The simulator, more fully described in Reference 5, uses the actual 98-degree inclination orbit together with precise models of the Earth's geomagnetic field, the horizon sensor, and the attitude control system. A variable stepsize, Adams-Moulton predictor-corrector algorithm was used to integrate the equations of motion. It was found that asymptotic stability, i.e., convergence of the wheel axis to within 10 degrees of the orbit normal, required that $k > 0$ and $h > 2I\omega_o > 0$ in agreement with the predictions of the model. Simulated results for the steady-state pitch rate were also in agreement with the model results illustrated in Figure 2.

MISSION-MODE CONTROL LAW

After the angular momentum vector has moved to within 10 degrees of the orbit normal and the pitch rate has reached the equilibrium value of approximately ω_o, the mission-mode control laws are invoked. Pitch capture and subsequent control* are obtained by torquing the momentum wheel in response to an error signal from the infrared horizon scanner (Reference 1).

Roll and yaw control is achieved by commanding the y-axis electromagnet based on magnetometer and roll-angle data (References 1 and 2). The electromagnet strength is commanded according to the control law

$$D_y = K_N \dot{B}_y + K_P B_x r \tag{25}$$

where $\vec{B}_B = (B_x, B_y, B_z)^T$ is the measured magnetic field in the body and K_P and K_N are the precession and nutation gain, respectively.† Substitution of

*The control requirements are $|p| < 1$ deg and $|\dot{p}| < 0.01$ deg/s.

†As for the acquisition-mode control, the hardware limitation $|D_y| < 10,000$ pole-cm is ignored.

Equations (1) and (12) into Equation (25) gives the mission-mode control torque

$$\vec{N}_B^C = \vec{D} \times \vec{B}$$

$$= \left\{ \left[k_n \left[\sin \omega_o t \, (2\dot{r} + y\omega_o) - \cos \omega_o t \, (\dot{y} - 2r\,\omega_o) \right] + k_p \cos \omega_o t \, r \right] \right\} \quad (26)$$

$$\times (2 \sin \omega_o t, \; 0, \; -\cos \omega_o t)^T$$

where the gains, magnetic field strength, and unit conversions have been absorbed into the constants k_n and k_p.

Substituting Equation (26) into Equation (14) and taking the Laplace transform leads to the coupled roll and yaw equations in matrix notations as*

$$M(S)\, L \begin{bmatrix} r \\ y \end{bmatrix} = L \begin{bmatrix} N_{Ex} \\ N_{Ez} \end{bmatrix} \quad (27a)$$

where

$$M(S) = \begin{bmatrix} I_x S^2 - 4k_n S \sin^2 \lambda + [4\omega_o^2 (I_y - I_z) + h\omega_o - \sin 2\lambda \, (2k_n \omega_o + k_p)] & [h - (I_x - I_y + I_z)\,\omega_o + k_n \sin 2\lambda] S - 2k_n \omega_o \sin^2 \lambda \\ [(I_z + I_x - I_y)\,\omega_o - h + k_n \sin 2\lambda] S + (k_p + 2\omega_o k_n) \cos^2 \lambda & I_z S^2 - k_n S \cos^2 \lambda + (I_y - I_x)\,\omega_o^2 + h\omega_o + k_n \omega_o \sin 2\lambda / 2 \end{bmatrix} \quad (27b)$$

and $\lambda = \omega_o t$ is a measure of latitude.** Although many approximations were employed in obtaining Equation (27), and simulations using detailed hardware

---

* Here, the moment of inertia tensor is assumed to be diagonal with principal moments I_X, I_y, and I_Z. Gravity gradient disturbance torques are included in the left-hand side of Equation (27).

**For $|\lambda| \leq 90$ deg, λ is the subsatellite latitude (a minus sign denotes the southern hemisphere); for $|\lambda| > 90$ deg, $180-\lambda$ is the subsatellite latitude.

and environmental models (particularly for the magnetic field) are required to evaluate the control system performance, most of the characteristics of the HCMM on-orbit control system are contained in the relatively simple model described by Equation (27). For a given latitude and control gains, the zeros of the characteristic equation

$$\det (M(S)) = 0 \tag{28}$$

may be computed. In general, there are four roots to the fourth-order Equation (28). In the absence of control torques, these roots are purely imaginary $\pm i\omega_n$ and $\pm i\omega_o$, where $\omega_n \approx h/\sqrt{I_X I_Z}$ is the nutation frequency and ω_o is the orbital frequency. With nutation control, but no precession control ($k_n < 0$, $k_p = 0$), the roots are complex conjugate pairs with negative real parts, and the system is damped and stable. The nutation damping time constant, τ_n, is shown as a function of latitude in Figure 3; at the equator (λ=0) $\tau_n \approx -0.6/k_n$.

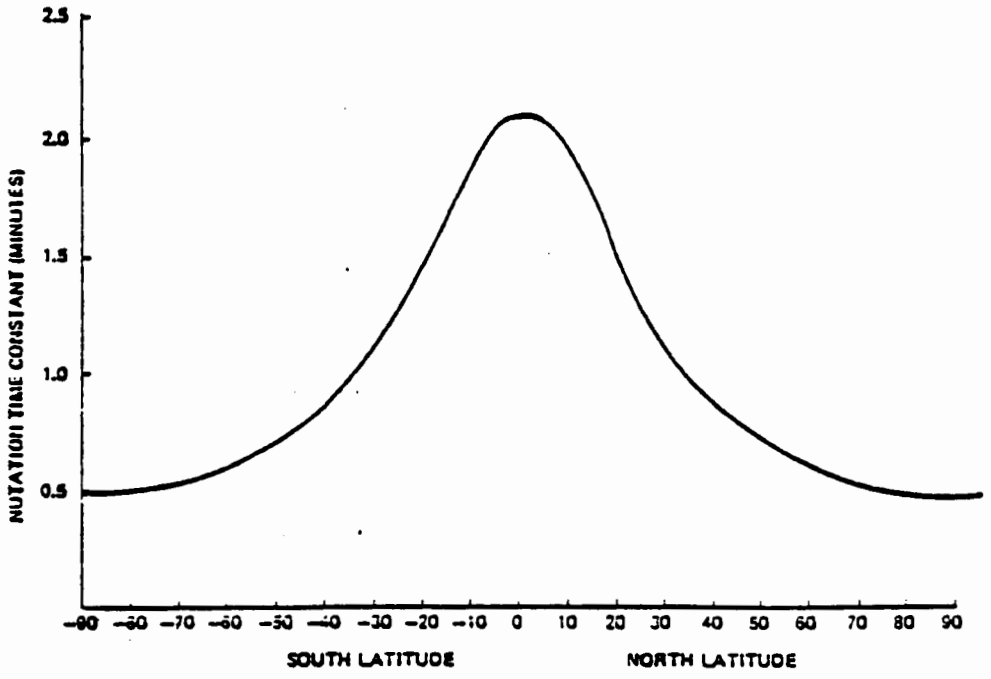

Fig. 3 HCMM Damping Time Constants for $k_n = -0.33$ J·s and $k_p = -0.011$ J

Routh's criteria may be applied to Equation (28) to obtain the necessary conditions for stable precession control as

$$\begin{aligned}&[4\omega_o^2 (I_y - I_z) + h\omega_o - \sin 2\lambda\,(2k_n \omega_o + k_p)]\\ &\times [\omega_o^2 (I_y - I_z) + h\omega_o + \tfrac{1}{2} k_n \omega_o \sin 2\lambda]\\ &+ \tfrac{1}{2} k_n \omega_o \sin^2 2\lambda\,(2k_n \omega_o + k_p) > 0\end{aligned} \tag{29a}$$

$$\begin{aligned}&-4k_n \sin^2\lambda\,[(I_y - I_x)\,\omega_o^2 + h\omega_o + \tfrac{1}{2} k_n \omega_o \sin 2\lambda]\\ &- k_n \cos^2\lambda\,[4(I_y - I_z)\,\omega_o^2 + h\omega_o - (2k_n \omega_o + k_p) \sin 2\lambda]\\ &- 2k_n \omega_o \sin^2\lambda\,[(I_y - I_x - I_z)\,\omega_o + h - k_n \sin 2\lambda]\\ &- (2k_n \omega_o + k_p) \cos^2\lambda\,[(I_y - I_x - I_z)\,\omega_o + h + k_n \sin 2\lambda]\end{aligned} \tag{29b}$$

$$k_n < 0 \tag{29c}$$

For HCMM,

$$\begin{aligned}&h >> |4(I_y - I_z)\,\omega_o|\\ &h >> |(I_y - I_x)\,\omega_o|\\ &|k_p| >> |2k_n \omega_o|\end{aligned} \tag{30}$$

and Equation (29) may be rewritten to good approximation as

$$h\omega_o - k_p \sin 2\lambda > 0 \tag{31a}$$

$$-k_n \omega_o\,(6 \tan^2\lambda + 1) - k_p > 0 \tag{31b}$$

$$k_n < 0 \tag{31c}$$

In Fig. 4, the dotted line shows that the mission attitude (pitch = roll= yaw = 0) is a position of stable equilibrium even in the absence of active precession control although the time constant is too long (~ 120 minutes) to counter the effect of typical disturbance torques. The dashed line shows the precession time constant for the control law defined by Equation (25). For the HCMM parameters, this precession control law is ineffective in the southern hemisphere and unstable between 14 and 76 degrees south latitude when the spacecraft is traveling north. (The northern hemisphere is the region of ineffective control system performance when the spacecraft is traveling south.)

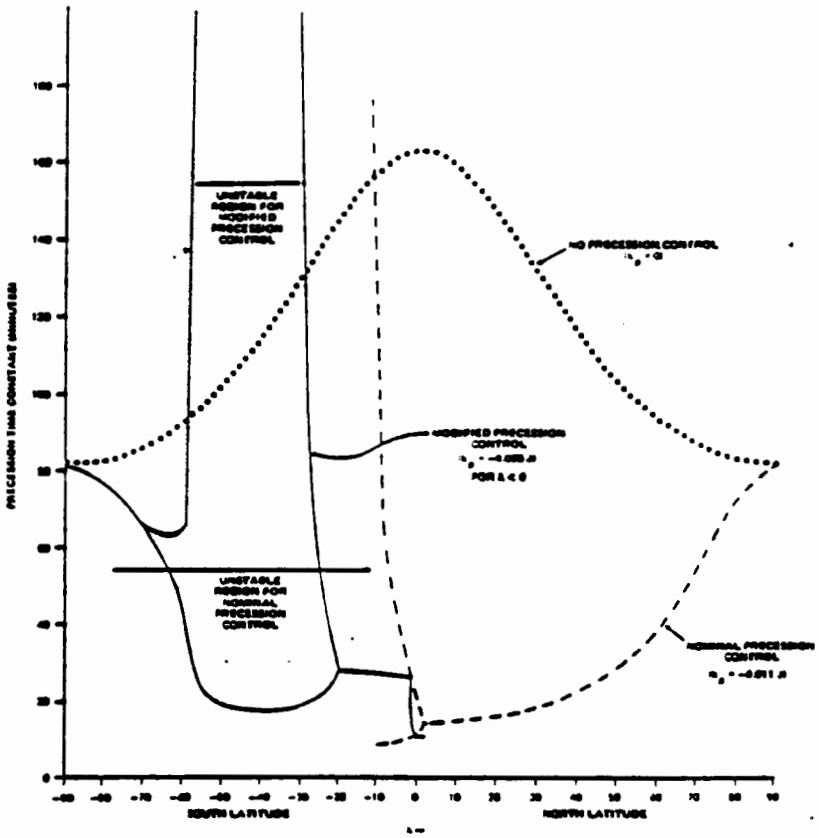

Fig. 4 Precession Control Time Constant as a Function of Latitude (Spacecraft is Traveling North)

Consequently, the HCMM control system deactivates precession and nutation control (i.e. sets $k_n = k_p = 0$) whenever $|B_z/B_x| > 1.4$. This "magnetic blanking" results in active control only within about 35 degrees of the equator. Equation 31 suggests that a more effective procedure might be to decrease the magnitude of k_p when $\sin 2\lambda < 0$, viz. when $B_x B_z < 0$. The solid line in Fig. 4 shows the precession time constants that result from modifying the control law by halving the precession gain when $B_x B_z < 0$. This modification extends the region of effective precession control to 20 degrees latitude and limits the unstable region to between 35 and 55 degrees south (north) latitude when the spacecraft is traveling north (south). Detailed parametric studies can thus be conducted to establish near optimal gains and control laws and to obtain regions of stability by solving algebraic equations without the need for time-consuming simulation.

The simulator was used to compare the performance of the modified and nominal HCMM control laws and to validate the predictions of the model. Fig. 5 compares the response of the two control laws to a 5-degree roll angle error. Note the extended periods of magnetic blanking for the nominal control law and the brief periods of ineffective control for the modified control law.

Although the response of the modified control law to transient errors is excellent, numerical simulations of steady-state conditions showed substantially poorer performance than the nominal control law. This result indicated the inadequacies of the simplified model using a polar orbit and dipole magnetic field at high latitudes. Consequently, magnetic blanking, with $|B_z/B_x| > 2$, and an increased precession gain, with $k_p = -0.022J$, were incorporated into the modified control law to avoid counterproductive torquing at latitudes above 45 degrees where the model is inadequate. The performance of this control law is somewhat better than the nominal control law; however, additional simulations and analysis are required to make a definitive comparison of the two control laws and to obtain optimum control law parameters.

These results demonstrate the need for both analytical and numerical studies in the design of attitude control laws and may be used to improve the attitude control performance of future, high-inclination AEM. Further analytical studies are also needed to optimize the attitude control performance of missions such as AEM-B, scheduled for launch in March 1979, at an orbital inclination of 50 degrees.

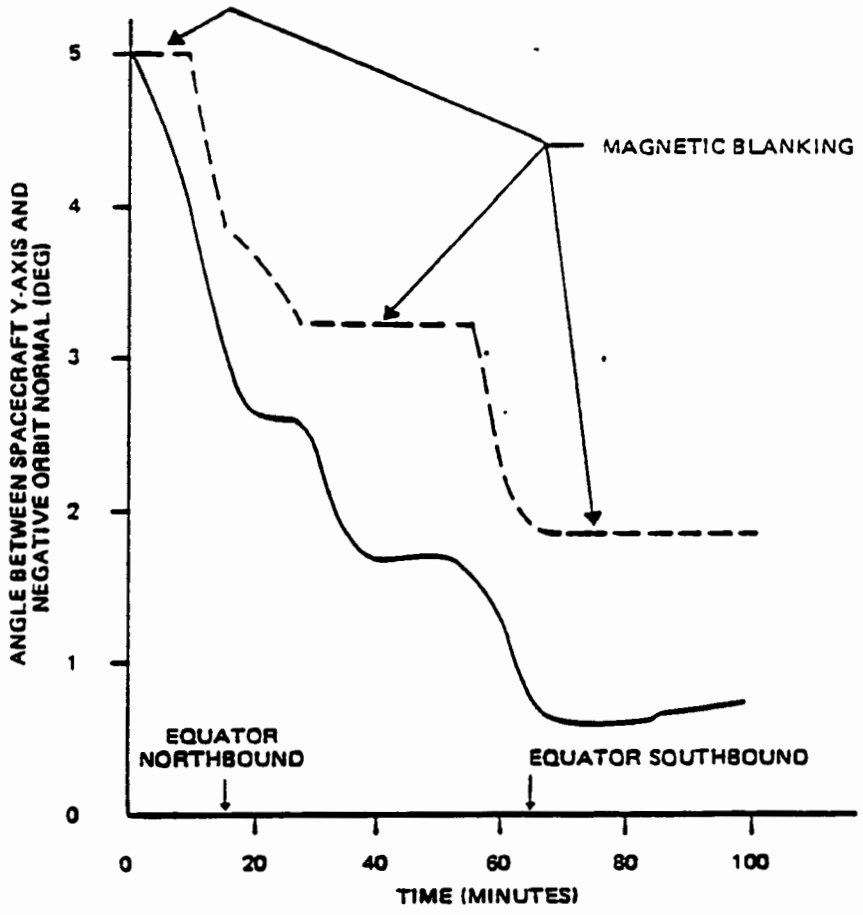

Fig. 5 Nominal (dashed line) and Modified (solid line) Control System Response to a 5-degree Roll Angle Error

APPENDIX

In this Appendix an analytical solution for the pitch rate as given by Equation (15b) is obtained. Recall that

$$\ddot{p}(t) + \frac{9k\,B^2}{2I}\left(\frac{5}{9} - \frac{1}{3}\cos 2\omega_o t\right)\dot{p}(t) + 2k\,B^2\,\omega_o = 0 \qquad \text{(A1)}$$

Straightforward application of the method of variation of parameters leads to the solution

$$\dot{p}(t) = \exp\left[-2\frac{\omega_1}{\omega_o}\left(\frac{5}{9}\omega_o t - \frac{1}{6}\sin 2\omega_o t\right)\right] \times \left\{\dot{p}(0) + \frac{8}{9}\omega_o\omega_1\int_0^t dt'\exp\left[2\frac{\omega_1}{\omega_o}\left(\frac{5}{9}\omega_o t - \frac{1}{6}\sin 2\omega_o t\right)\right]\right\} \qquad \text{(A-2)}$$

with

$$\omega_1 \equiv \frac{9kB^2}{4I} \qquad \text{(A-3)}$$

In the asymptotic limit this becomes in more compact notation,

$$\dot{p}_{ss}(t) \equiv \lim_{t\to-\infty}\dot{p}(t)$$

$$= \lim_{u\to-\infty}\left\{c\exp\left[-(au - b\sin u)\right]\int_o^u du'\exp\left[au' - b\sin u'\right]\right\}\omega_o \qquad \text{(A-4)}$$

where

$$a = \frac{5\,\omega_1}{9\,\omega_o}$$

$$b = \frac{\omega_1}{3\,\omega_o} \qquad \text{(A-5)}$$

$$c = \frac{4\,\omega_1}{9\,\omega_o}$$

$$u = 2\,\omega_o t$$

We may obtain the Fourier expansion of exp (b sin u) by noting (Reference 3) that

$$\exp(\pm b \sin s) = I_0(b) + 2\sum_{m=1}^{\infty} (-)^m I_{2m}(b) \cos 2ms$$

$$\pm 2\sum_{m=0}^{\infty} (-)^m I_{2m+1}(b) \sin(2m+1)\,s \qquad \text{(A-6)}$$

where $I_m(b)$ is the modified Bessel function of the first kind. Substituting Equation (A-6) into the integral in Equation (A-4), we obtain

$$\int_0^u \exp\,[au' - b \sin u']\,du' = \exp(au') \left\{ I_0(b)\frac{1}{a} \right.$$

$$+2\sum_{m=1}^{\infty} (-)^m \frac{I_{2m}(b)}{a^2 + (2m)^2}\,[a \cos 2mu' + 2m \sin 2mu'] \qquad \text{(A-7)}$$

$$\left. -2\sum_{m=0}^{\infty} (-)^m \frac{I_{2m+1}(b)}{a^2 + (2m+1)^2}\,[a \sin (2m+1)u' - (2m+1)\cos(2m+1)u'] \right\} \Bigg|_0^u$$

Only the contribution evaluated at the upper limit of the integral contributes to Equation (A-4).

It is obvious from our earlier observations (Equation (11)) that $\dot{p}_{ss}(t) = \omega_y^{ss} - \omega_0$ must tend toward an average value close to ω_0. We may isolate this constant term by noting that

$$\frac{a}{a^2 + n^2} = \frac{1}{a} - \frac{n^2}{a(a^2 + n^2)} \tag{A-8}$$

and recasting Equation (A-7) as

$$\int_0^u du' \exp[au' - b \sin u'] du'$$

$$= \frac{1}{a} \exp(au) \left\{ I_0(b) + 2 \sum_{m=1}^{\infty} (-)^m I_{2m}(b) \cos 2mu \right.$$

$$\left. -2 \sum_{m=0}^{\infty} (-)^m I_{2m+1}(b) \sin(2m + 1) u \right\} \tag{A-9}$$

$$+ \frac{1}{a} \exp(au) \left\{ 2 \sum_{m=1}^{\infty} (-)^m \frac{2m}{a^2 + (2m)^2} \left[\frac{-2m}{a} \cos 2mu + \sin 2mu \right] \right.$$

$$\left. + 2 \sum_{m=0}^{\infty} (-)^m \frac{2m + 1}{a^2 + (2m + 1)^2} \left[\frac{2m + 1}{a} \sin(2m + 1)u + \cos(2m + 1) u \right] \right\}$$

+ terms which remain bounded when $u \to \infty$.

The first term in Equation (A-9) is simply $\frac{1}{a}\exp[au - b\sin u]$. Thus, Equation (A-4) becomes

$$\dot{p}_{ss}(t) = \frac{4}{5}\omega_o\left[1 + \exp(b\sin u)\left\{2\sum_{m=1}^{\infty}(-)^m\frac{2m}{a^2+(2m)^2}\left[-\frac{2m}{a}\cos 2mu + \sin 2mu\right]\right.\right. \tag{A-10}$$
$$\left.\left. + 2\sum_{m=0}^{\infty}(-)^m\frac{2m+1}{a^2+(2m+1)^2}\left[\frac{2m+1}{a}\sin(2m+1)u + \cos(2m+1)u\right]\right\}\right]$$

It is now a simple matter to substitute Equation (A-6) into Equation (A-10) to obtain the Fourier series for $\dot{p}_{ss}(t)$. Of particular interest is the secular term, for which we obtain

$$\langle\dot{p}_{ss}\rangle = \frac{4}{5}\omega_o + \frac{8\omega_o}{5}\sum_{m=1}^{\infty}(-)^{m+1}\frac{m^2}{a^2+m^2}[I_m(b)]^2 \tag{A-11}$$

For $\omega_1 \to o$ (weak-coupling limit), the series appearing in Equation (A-11) also vanishes and, hence, $\langle\dot{p}_{ss}\rangle = \frac{4}{5}\omega_o$ in this limit. For $\omega_1 \to \infty$ (strong-coupling limit), the series appearing in Equation (A-11) can be evaluated most easily by expressing the quantities appearing in Equation (A-4) as a Taylor's series and integrating them. This leads to

$$\langle\dot{p}_{ss}\rangle = \frac{4\omega_o}{5}\left[1 + \sum_{n=1}^{\infty}(2b)^{2n}\prod_{m=1}^{n}\frac{(2m-1)}{2m[(2a)^2+(2m)^2]}\right] \tag{A-12}$$

In the limit $\omega_1 \to \infty$ (i.e., a and $b \to \infty$),

$$\langle \dot{p}_{ss} \rangle \to \frac{4\omega_o}{5}\left[1 + \frac{1}{2}\left(\frac{3}{5}\right)^2 + \frac{1\cdot 3}{2\cdot 4}\left(\frac{3}{5}\right)^4 + \frac{1\cdot 3\cdot 5}{2\cdot 4\cdot 6}\left(\frac{3}{5}\right)^6 + \ldots\right] \qquad \text{(A-13)}$$

$$= \frac{4\omega_o}{5}\left[1 - \left(\frac{3}{5}\right)^2\right]^{-1/2} = \omega_o$$

REFERENCES

1. A. C. Stickler and K. T. Alfriend, "Elementary Magnetic Attitude Control System," Journal of Spacecraft and Rockets, May 1976

2. M. G. Grell and W. H. Huang, AEM-A Attitude Control Contingency Study, Computer Sciences Corporation, CSC/TM-76/6203, October 1976

3. M. Abramowitz and I. A. Stegun, Handbook of Mathematical Functions, U.S. Government Printing Office, 1964

4. M. H. Kaplan, Modern Spacecraft Dynamics and Control, New York: John Wiley and Sons, 1976

5. S. G. Hotovy et. al., Applications Explorer Missions-A/Heat Capacity Mapping Mission (AEM-A/HCMM) Attitude System Functional Specifications and Requirements, CSC/SD-77/6017, January 1977